
Disentangling Disentanglement in Variational Auto-Encoders

Emile Mathieu^{*1} Tom Rainforth^{*1} N. Siddharth^{*2} Yee Whye Teh¹

Abstract

We develop a generalisation of disentanglement in variational auto-encoders (VAEs)—*decomposition* of the latent representation—characterising it as the fulfilment of two factors: a) the latent encodings of the data having an appropriate level of overlap, and b) the aggregate encoding of the data conforming to a desired structure, represented through the prior. Decomposition permits disentanglement, i.e. explicit independence between latents, as a special case, but also allows for a much richer class of properties to be imposed on the learnt representation, such as sparsity, clustering, independent subspaces, or even intricate hierarchical dependency relationships. We show that the β -VAE varies from the standard VAE predominantly in its control of latent overlap and that for the standard choice of an isotropic Gaussian prior, its objective is invariant to rotations of the latent representation. Viewed from the decomposition perspective, breaking this invariance with simple manipulations of the prior can yield better disentanglement with little or no detriment to reconstructions. We further demonstrate how other choices of prior can assist in producing different decompositions and introduce an alternative training objective that allows the control of both decomposition factors in a principled manner.

1. Introduction

An oft-stated motivation for learning disentangled representations of data with deep generative models is a desire to achieve interpretability (Bengio et al., 2013; Chen et al., 2016b)—particularly the *decomposability* (see §3.2.1 in Lipton, 2016) of latent representations to admit intuitive explanations. Most work on disentanglement has constrained the form of this decomposition to capturing purely *independent* factors of variation (Alemi et al., 2017; Ansari and Soh, 2018; Burgess et al., 2018; Chen et al., 2018; 2016b;

Eastwood and Williams, 2018; Esmaeili et al., 2018; Higgins et al., 2016; Kim and Mnih, 2018; Xu and Durrett, 2018; Zhao et al., 2017), typically evaluating this using purpose-built, synthetic data (Chen et al., 2018; Eastwood and Williams, 2018; Higgins et al., 2016; Kim and Mnih, 2018), whose generative factors are independent by construction. However, the high-level motivation for achieving decomposability places no a priori constraints on the form of the decompositions—just that they are captured effectively.

The conventional view of disentanglement, as recovering independence, has subsequently motivated the development of formal evaluation metrics for independence (Eastwood and Williams, 2018; Kim and Mnih, 2018), which in turn has driven the development of objectives that target these metrics, often by employing regularisers explicitly encouraging independence in the representations (Eastwood and Williams, 2018; Esmaeili et al., 2018; Kim and Mnih, 2018).

We argue that such an approach is not generalisable, and potentially even harmful, to learning decomposable representations for more complicated problems, where such simplistic representations cannot accurately mimic the generation of high dimensional data from low dimensional latent spaces, and more richly structured dependencies are required.

To this end, we posit a generalisation of disentanglement—*decomposing* latent representations—that can help avoid such pitfalls. We characterise decomposition as the fulfilment of two factors: a) the latent encodings of data having an appropriate level of overlap, and b) the aggregate encoding of data conforming to a desired structure, represented through the prior. We emphasize that neither of these factors are sufficient in isolation: without an appropriate level of overlap, encodings can degrade to a lookup table where the latents convey little information about the data, and without the aggregate encoding of the data following a desired structure, we do not achieve the desired type of decomposition.

The typical disentanglement assumption of independence *implicitly* makes a choice of decomposition—that the latent features are independent of one another. We make this *explicit*, and exploit it to provide improvement to disentanglement simply through judicious choices of structure in the prior, while also introducing a framework flexible enough to capture alternate, more complex, notions of decomposition such as sparsity, clustering, hierarchical structuring, or

^{*}Equal contribution ¹Department of Statistics, University of Oxford, United Kingdom ²Department of Engineering, University of Oxford, United Kingdom. Correspondence to: Emile Mathieu <emile.mathieu@stats.ox.ac.uk>, Tom Rainforth <rainforth@stats.ox.ac.uk>, N. Siddharth <nsid@robots.ox.ac.uk>.

independent subspaces.

To connect our framework with existing approaches for encouraging disentanglement, we provide a theoretical analysis of the β -VAE (Alemi et al., 2018; 2017; Higgins et al., 2016), and show that it typically only allows control of latent overlap, the first decomposition factor. We show that it can be interpreted, up to a constant offset, as the standard VAE objective with its prior annealed as $p_\theta(\mathbf{z})^\beta$ and an additional maximum entropy regularization of the encoder that increases the stochasticity of the encodings. Specialising this result for the typical choice of a Gaussian encoder and isotropic Gaussian prior indicates that the β -VAE, up to a scaling of the latent space, is equivalent to the VAE plus a regulariser encouraging higher encoder variance. Moreover, this objective is invariant to rotations of the learned latent representation, meaning that it does not encourage the latent variables to take on meaningful representations any more than an arbitrary rotation of them.

We confirm these results empirically, while further using our decomposition framework to show that simple manipulations to the prior can improve disentanglement, and other decompositions, with little or no detriment to the reconstruction accuracy. Further, motivated by our analysis, we propose an alternative objective that takes into account the distinct needs of the two factors of decomposition, and use it to learn clustered and sparse representations as demonstrations of alternative forms of decomposition.

2. Background and Related Work

We begin with a brief review of VAEs and an overview of prior work on disentanglement.

2.1. Variational Auto-Encoders

Let \mathbf{x} be an \mathcal{X} -valued random variable distributed according to an unknown generative process with density $p_{\mathcal{D}}(\mathbf{x})$ from which we have observations, $X = \{\mathbf{x}_1, \dots, \mathbf{x}_n\}$. The aim is to learn a latent-variable model $p_\theta(\mathbf{x}, \mathbf{z})$ that captures this generative process, comprising of a fixed¹ prior over latents $p(\mathbf{z})$ and a parametric likelihood $p_\theta(\mathbf{x}|\mathbf{z})$. Learning proceeds by minimising a divergence between the true data generating distribution and the model w.r.t θ , typically

$$\arg \min_{\theta} \text{KL}(p_{\mathcal{D}}(\mathbf{x}) \parallel p_\theta(\mathbf{x})) = \arg \max_{\theta} \mathbb{E}_{p_{\mathcal{D}}(\mathbf{x})} [\log p_\theta(\mathbf{x})]$$

where $p_\theta(\mathbf{x}) = \int_{\mathcal{Z}} p_\theta(\mathbf{x} | \mathbf{z}) p(\mathbf{z}) d\mathbf{z}$ is the marginal likelihood, or evidence, of datapoint \mathbf{x} under the model, approximated by averaging over the observations.

However, estimating $p_\theta(\mathbf{x})$ (or its gradients) to any sufficient degree of accuracy is typically infeasible. A common

¹Sometimes one may also wish to learn parameters of the prior, but we omit consideration of this for simplicity.

strategy to ameliorate this issue involves the introduction of a parametric inference model $q_\phi(\mathbf{z}|\mathbf{x})$ to construct a variational evidence lower bound (ELBO) on $\log p_\theta(\mathbf{x})$ as follows

$$\begin{aligned} \mathcal{L}(\mathbf{x}; \theta, \phi) &\triangleq \log p_\theta(\mathbf{x}) - \text{KL}(q_\phi(\mathbf{z}|\mathbf{x}) \parallel p_\theta(\mathbf{z}|\mathbf{x})) \\ &= \mathbb{E}_{q_\phi(\mathbf{z}|\mathbf{x})} [\log p_\theta(\mathbf{x}|\mathbf{z})] - \text{KL}(q_\phi(\mathbf{z}|\mathbf{x}) \parallel p(\mathbf{z})). \end{aligned} \quad (1)$$

A variational auto-encoder (VAE) (Kingma and Welling, 2014; Rezende et al., 2014) views this objective from the perspective of a deep stochastic auto-encoder, taking the inference model $q_\phi(\mathbf{z}|\mathbf{x})$ to be an encoder and the likelihood model $p_\theta(\mathbf{x}|\mathbf{z})$ to be a decoder, where θ and ϕ are neural network parameters, and where learning happens via stochastic gradient ascent (SGA) using unbiased estimates of $\nabla_{\theta, \phi} \frac{1}{n} \sum_{i=1}^n \mathcal{L}(\mathbf{x}_i; \theta, \phi)$. Note that when clear from the context, we simply denote $\mathcal{L}(\mathbf{x}; \theta, \phi)$ as $\mathcal{L}(\mathbf{x})$.

2.2. Disentanglement

Disentanglement, as typically employed in literature, refers to independence among features in a representation (Bengio et al., 2013; Eastwood and Williams, 2018; Higgins et al., 2018). Conceptually, however, it has a long history, far longer than we could reasonably do justice here, and is far from specific to VAEs. The idea stems back to traditional methods such as ICA (Hyvärinen and Oja, 2000; Yang and Amari, 1997) and conventional auto-encoders (Schmidhuber, 1992), through to a range of modern approaches employing deep learning (Achille and Soatto, 2019; Chen et al., 2016a; Cheung et al., 2014; Hjelm et al., 2018; Makhzani et al., 2015; Mathieu et al., 2016; Reed et al., 2014).

Of particular relevance to this work are approaches that explore disentanglement in the context of VAEs (Alemi et al., 2017; Chen et al., 2018; Esmaeili et al., 2018; Higgins et al., 2016; Kim and Mnih, 2018; Siddharth et al., 2017). Here one aims to achieve independence between the dimensions of the aggregate encoding, typically defined as $q_\phi(\mathbf{z}) \triangleq \mathbb{E}_{p_{\mathcal{D}}(\mathbf{x})} [q(\mathbf{z}|\mathbf{x})] \approx \frac{1}{n} \sum_{i=1}^n q(\mathbf{z}|\mathbf{x}_n)$. The significance of $q_\phi(\mathbf{z})$ is that it is the marginal distribution induced on the latents by sampling a datapoint and then using the encoder to sample an encoding given that datapoint. It can thus informally be thought of as the distribution for “sampling” representations.

Within the disentangled VAEs literature, there is also a distinction between unsupervised approaches, and semi-supervised approaches, where one knows the true generative factors for some subset of data (Bouchacourt et al., 2018; Kingma et al., 2014; Siddharth et al., 2017). Our focus however is on the unsupervised setting.

Much of the prior work in the field has either implicitly or explicitly presumed a slightly more ambitious definition of disentanglement than considered above: that it is a measure of how well one captures *true* factors of variation (which

happen to be independent by construction for synthetic data), rather than just independent factors. After all, if we wish for our learned representations to be interpretable, it is necessary for the latent variables to take on clear-cut meaning.

One such definition is given by Eastwood and Williams (2018), who define it as the extent to which a latent dimension $d \in D$ in a representation predicts a true generative factor $k \in K$, with each latent capturing at most one generative factor. This implicitly assumes $D \geq K$, as otherwise the latents are unable to explain all the true generative factors. However, for real data, the association is more likely $D \ll K$, with one learning a low-dimensional abstraction of a complex process involving many factors. Consequently, such simplistic representations cannot, by definition, be found for more complex datasets that require more richly structured dependencies to be able to encode the information required to generate higher dimensional data. Moreover, for complex datasets involving a finite set of datapoints, it might not be reasonable to presume that one could capture the elements of the true generative process—the data itself might not contain sufficient information to recover these and even if it does, the computation required to achieve this through model learning is unlikely to be tractable.

The subsequent need for richly structured dependencies between latent dimensions has been reflected in the motivation for a handful of approaches (Bouchacourt et al., 2018; Esmaeili et al., 2018; Johnson et al., 2016; Siddharth et al., 2017) that explore this through graphical models, although employing mutually-inconsistent, and not generalisable, interpretations of disentanglement. This motivates our development of a decomposition framework as a means of extending beyond the limitations of disentanglement.

3. Decomposition: A Generalisation of Disentanglement

The commonly assumed notion of disentanglement is quite restrictive for complex models where the true generative factors are not independent, very large in number, or where it cannot be reasonably assumed that there is a well-defined set of “true” generative factors (as will be the case for many, if not most, real datasets). To this end, we introduce a generalization of disentanglement, *decomposition*, which at a high-level can be thought of as imposing a desired structure on the learned representations. This permits disentanglement as a special case, for which the desired structure is that $q_\phi(z)$ factors along its dimensions.

We characterise the decomposition of latent spaces in VAEs to be the fulfilment of two factors (as shown in Figure 1):

- An “appropriate” level of overlap in the latent space—ensuring that the range of latent values capable of encoding a particular datapoint is neither too small, nor too

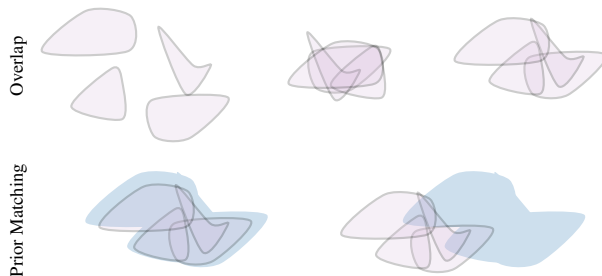


Figure 1. The two factors of decomposition. [Top] Overlap between encodings $q_\phi(z | x_i)$, showing cases with (l) too little overlap, (m) too much overlap, and (r) an “appropriate” level of overlap. [Bottom] Illustration of (l) good and (r) bad regularisation between the aggregate posterior $q_\phi(z)$ and the desired prior $p(z)$.

large. This is, in general, dictated by the level of stochasticity in the encoder: the higher the encoder variance, the higher the number of datapoints which can plausibly give rise to a particular encoding.

- The aggregate encoding $q_\phi(z)$ matching the prior $p_\theta(z)$, where the latter expresses the desired dependency structure between latents.

The overlap factor (a) is perhaps best understood by considering extremes—too little, and the latents effectively become a lookup table; too much, and the data and latents don’t convey information about each other. In either case, meaningfulness of the latent encodings is lost. Thus, without the *appropriate* level of overlap—dictated both by noise in the true generative process and dataset size—it is not possible to enforce meaningful structure on the latent space.

The regularisation factor (b) enforces a congruence between the (aggregate) latent embeddings of data and the dependency structures expressed in the prior. We posit that such structure is best expressed in the prior, as opposed to explicit independence regularisation of the marginal posterior (Chen et al., 2018; Kim and Mnih, 2018), to enable the *generative* model to express the desired decomposition, and to avoid potentially violating the self-consistency between encoder, decoder, and true data generating distributions. The prior also provides a rich and flexible means of expressing desired structure by defining a generative process that encapsulates dependencies between variables, as with a graphical model.

Critically, *neither factor is sufficient in isolation*. An inappropriate level of overlap in the latent space will impede interpretability, irrespective of quality of regularisation, as the latent space need not be meaningful. Conversely, without the pressure to regularise to the prior, the latent space is under no constraint to exhibit the desired structure.

Decomposition is inherently subjective as we must choose the structure of the prior we regularize to depending on how we intend to use our learned model or what kind of features we would like uncover from the data. This may at first seem unsatisfactory compared to the seemingly objective adjust-

ments often made to the ELBO by disentanglement methods. However, disentanglement is itself a subjective choice for the decomposition. We can embrace this subjective nature through judicious choices of the prior distribution; ignoring this imposes unintended assumptions which can have unwanted effects. For example, as we will later show, the rotational invariance of the standard prior $p(\mathbf{z}) = \mathcal{N}(\mathbf{z}; 0, I)$ provides no assistance towards disentanglement.

3.1. Characterizing Overlap

Precisely formalising what constitutes overlap in the latent space is surprisingly subtle. Prior work has typically characterised it in terms of the mutual information $I(\mathbf{x}; \mathbf{z})$ between data and latents (Alemi et al., 2018; 2017; Hoffman and Johnson, 2016; Phuong et al., 2018). Although $I(\mathbf{x}; \mathbf{z})$ provides a perfectly serviceable characterisation of overlap in a number of cases, it is not universally applicable. In particular, if the form of the encoding distribution is not fixed, as when employing normalising flows, for example, $I(\mathbf{x}; \mathbf{z})$ would not necessarily characterise overlap well.

Consider for example, an encoding distribution that was a mixture between a uniform distribution on a tiny ϵ -ball around the mean encoding $\mu_\phi(x)$ and the prior as $q_\phi(\mathbf{z}|\mathbf{x}) = \lambda \cdot \text{Uniform}(\|\mu_\phi(x) - \mathbf{z}\|_2 < \epsilon) + (1 - \lambda) \cdot p(\mathbf{z})$ and that the encoder and decoder were sufficiently flexible to learn arbitrary representations. One could arrive at *any* value for mutual information simply by an appropriate choice of λ . However, enforcing structuring of the latent space will be effectively impossible due the lack of any pressure (other than a potentially small amount from internal regularization in the encoder network itself) for similar encodings to correspond to similar datapoints; the overlap between any two encodings is the same unless they are within ϵ of each other.

While this example is a bit contrived, it highlights two features of overlap that $I(\mathbf{x}; \mathbf{z})$ fails to capture. Firstly, it does not capture *how many* other datapoints one datapoint’s encoding overlaps with—in the context of imposing structure, there is an important distinction between having large overlap with a small number of other datapoints and small overlap with a large number of other datapoints—both of which potentially having the same mutual information. Secondly, it fails to account for a notion of *locality* in the latent space—if the encoding distribution is heavily multimodal, then even if the encoder entropy is low, there could be many regions of the space a point can be encoded to, undermining our ability to impose structure in a meaningful manner.

Thankfully, when the encoder is unimodal with fixed form (in particular that the tail behavior is fixed) and the prior is well-characterized by Euclidean distances, then these factors have a substantially reduced ability to vary for a given $I(\mathbf{x}; \mathbf{z})$, which subsequently becomes a good characterization of the level of overlap. When $q_\phi(\mathbf{z}|\mathbf{x})$ is Gaussian,

controlling the variance of $q_\phi(\mathbf{z}|\mathbf{x})$ (with a fixed $q_\phi(\mathbf{z})$) should similarly provide an effective means of achieving the desired overlap behavior. As this is the most common use case, we leave development of more a general definition of overlap to future work, simply noting that this is an important consideration when using flexible encoder distributions.

4. Deconstructing the β -VAE

To connect existing approaches to our proposed framework, we now consider, as a case study, the β -VAE (Higgins et al., 2016)—an adaptation of the VAE objective (ELBO) to learn better-disentangled representations. Specifically, it scales the KL term in the standard ELBO by a factor $\beta > 1$ as

$$\mathcal{L}_\beta(\mathbf{x}) = \mathbb{E}_{q_\phi(\mathbf{z}|\mathbf{x})}[\log p_\theta(\mathbf{x}|\mathbf{z})] - \beta \text{KL}(q_\phi(\mathbf{z}|\mathbf{x}) \| p_\theta(\mathbf{z})). \quad (2)$$

Hoffman et al. (2017) showed that the β -VAE target can be viewed as a standard ELBO with the alternative prior $r(\mathbf{z}) \propto q_\phi(\mathbf{z})^{(1-\beta)} p(\mathbf{z})^\beta$, along with terms involving the mutual information and the prior’s normalising constant.

We now introduce an alternate deconstruction as follows

Theorem 1. *The β -VAE target $\mathcal{L}_\beta(\mathbf{x})$ can be interpreted in terms of the standard ELBO, $\mathcal{L}(\mathbf{x}; \pi_{\theta,\beta}, q_\phi)$, for an adjusted target $\pi_{\theta,\beta}(\mathbf{x}, \mathbf{z}) \triangleq p_\theta(\mathbf{x} | \mathbf{z}) f_\beta(\mathbf{z})$ with annealed prior $f_\beta(\mathbf{z}) \triangleq p_\theta(\mathbf{z})^\beta / F_\beta$ as*

$$\mathcal{L}_\beta(\mathbf{x}) = \mathcal{L}(\mathbf{x}; \pi_{\theta,\beta}, q_\phi) + (\beta - 1)H_{q_\phi} + \log F_\beta \quad (3)$$

where $F_\beta \triangleq \int_{\mathbf{z}} p_\theta(\mathbf{z})^\beta d\mathbf{z}$ is constant given β , and H_{q_ϕ} is the entropy of $q_\phi(\mathbf{z} | \mathbf{x})$.

Proof. Starting with (2), we have

$$\begin{aligned} \mathcal{L}_\beta(\mathbf{x}) &= \mathbb{E}_{q_\phi(\mathbf{z}|\mathbf{x})}[\log p_\theta(\mathbf{x} | \mathbf{z})] + \beta H_{q_\phi} \\ &\quad + \beta \mathbb{E}_{q_\phi(\mathbf{z}|\mathbf{x})}[\log p_\theta(\mathbf{z})] \\ &= \mathbb{E}_{q_\phi(\mathbf{z}|\mathbf{x})}[\log p_\theta(\mathbf{x} | \mathbf{z})] + (\beta - 1)H_{q_\phi} + H_{q_\phi} \\ &\quad + \mathbb{E}_{q_\phi(\mathbf{z}|\mathbf{x})}[\log p_\theta(\mathbf{z})^\beta - \log F_\beta] + \log F_\beta \\ &= \mathbb{E}_{q_\phi(\mathbf{z}|\mathbf{x})}[\log p_\theta(\mathbf{x} | \mathbf{z})] + (\beta - 1)H_{q_\phi} \\ &\quad - \text{KL}(q_\phi(\mathbf{z} | \mathbf{x}) \| f_\beta(\mathbf{z})) + \log F_\beta \\ &= \mathcal{L}(\mathbf{x}; \pi_{\theta,\beta}, q_\phi) + (\beta - 1)H_{q_\phi} + \log F_\beta \end{aligned}$$

as required. \square

Clearly, the second term in (3), enforcing a maximum entropy regulariser on the posterior $q_\phi(\mathbf{z} | \mathbf{x})$, allows the value of β to affect the overlap of encodings in the latent space. We thus see that it provides a means of controlling decomposition factor (a). However, it is itself not sufficient to enforce disentanglement. For example, the entropy of $q_\phi(\mathbf{z} | \mathbf{x})$ is independent of its mean $\mu_\theta(\mathbf{x})$ and is independent to rotations of \mathbf{z} , so it is clearly incapable of discouraging certain

representations with poor disentanglement. All the same, having the wrong level of regularization can, in turn, lead to an inappropriate level of overlap and undermine the ability to disentangle. Consequently, this term is still important.

Although the precise impact of prior annealing depends on the original form of the prior, the high-level effect is the same—larger values of β cause the effective latent space to collapse towards the modes of the prior. For uni-modal priors, the main effect of annealing is to reduce the scaling of \mathbf{z} ; indeed this is the only effect for generalized Gaussian distributions. While this would appear not to have any tangible effects, closer inspection suggests otherwise—it ensures that the scaling of the encodings matches that of the prior. Only incorporating the maximum-entropy regularization will simply cause the scaling of the latent space to increase. The rescaling of the prior now cancels this effect, ensuring the scaling of $q_\phi(\mathbf{z})$ matches that of $p(\mathbf{z})$.

Taken together, this implies that the β -VAE’s ability to encourage disentanglement is predominantly through *direct* control over the level of overlap. It places no other direct constraint on the latents to disentangle (although in some cases, the annealed prior may inadvertently encourage better disentanglement), but instead helps avoid the pitfalls of inappropriate overlap. Amongst other things, this explains why large β is not universally beneficial for disentanglement, as the level of overlap can be increased too far.

4.1. Special Case – Gaussians

We gain further insights into the β -VAE in the common use case—assuming a Gaussian prior, $p(\mathbf{z}) = \mathcal{N}(\mathbf{z}; 0, \Sigma)$, and Gaussian encoder, $q_\phi(\mathbf{z} | \mathbf{x}) = \mathcal{N}(\mathbf{z}; \mu_\phi(\mathbf{x}), S_\phi(\mathbf{x}))$. It is straightforward to see that annealing simply scales the latent space by $1/\sqrt{\beta}$, i.e. $f_\beta(\mathbf{z}) = \mathcal{N}(\mathbf{z}; 0, \Sigma/\beta)$. Given this, it is easy to see that a VAE trained with the adjusted target $\mathcal{L}(\mathbf{x}; \pi_{\theta, \beta}, q_\phi)$, but appropriately scaling the latent space, will behave identically to one trained with the original target $\mathcal{L}(\mathbf{x})$. It will also have an identical ELBO as the expected reconstruction is trivially the same, while the KL between Gaussians is invariant to scaling both equally. More precisely, we have the following result.

Corollary 1. *If $p_\theta(\mathbf{z}) = \mathcal{N}(\mathbf{z}; 0, \Sigma)$ and $q_\phi(\mathbf{z} | \mathbf{x}) = \mathcal{N}(\mathbf{z}; \mu_\phi(\mathbf{x}), S_\phi(\mathbf{x}))$, then,*

$$\mathcal{L}_\beta(\mathbf{x}; \theta, \phi) = \mathcal{L}(\mathbf{x}; \theta', \phi') + \frac{(\beta - 1)}{2} \log |S_{\phi'}(\mathbf{x})| + c \quad (4)$$

where θ' and ϕ' represent rescaled networks such that

$$\begin{aligned} p_{\theta'}(\mathbf{x} | \mathbf{z}) &= p_\theta(\mathbf{x} | \mathbf{z}/\sqrt{\beta}), \\ q_{\phi'}(\mathbf{z} | \mathbf{x}) &= \mathcal{N}(\mathbf{z}; \mu_{\phi'}(\mathbf{x}), S_{\phi'}(\mathbf{x})), \\ \mu_{\phi'}(\mathbf{x}) &= \sqrt{\beta} \mu_\phi(\mathbf{x}), \\ S_{\phi'}(\mathbf{x}) &= \beta S_\phi(\mathbf{x}), \end{aligned}$$

and $c \triangleq \frac{D(\beta-1)}{2} \left(1 + \log \frac{2\pi}{\beta}\right) + \log F_\beta$ is a constant, with D denoting the dimensionality of \mathbf{z} .

Proof. See Appendix A. \square

Noting that c is irrelevant to the training process, this indicates an equivalence, up to scaling of the latent space, between training with the β -VAE objective and a maximum-entropy regularised version of the standard ELBO

$$\mathcal{L}_{H, \beta}(\mathbf{x}) \triangleq \mathcal{L}(\mathbf{x}) + \frac{(\beta - 1)}{2} \log |S_\phi(\mathbf{x})|, \quad (5)$$

whenever $p_\theta(\mathbf{z})$ and $q_\phi(\mathbf{z} | \mathbf{x})$ are Gaussian. Note that we implicitly presume suitable adjustment of neural-network hyper-parameters and the stochastic gradient scheme to account for the change of scaling in the optimal networks.

More formally we have the following, showing equivalence of all the stationary points for the two objectives.

Corollary 2. *Let $[\theta', \phi'] = g_\beta([\theta, \phi])$ represent the transformation required to produced the rescaled networks in Corollary 1. If $0 < |\det \nabla_{\theta, \phi} g([\theta, \phi])| < \infty \forall [\theta, \phi]$, then*

$$\nabla_{\theta, \phi} \mathcal{L}_\beta(\mathbf{x}; \theta, \phi) = \mathbf{0} \Leftrightarrow \nabla_{\theta', \phi'} \mathcal{L}_{H, \beta}(\mathbf{x}; \theta', \phi') = \mathbf{0}.$$

Thus $[\theta^*, \phi^*]$ being a stationary point of $\frac{1}{n} \sum_{i=1}^n \mathcal{L}_\beta(\mathbf{x}_i; \theta, \phi)$ indicates that $g_\beta([\theta^*, \phi^*])$ is a stationary point of $\frac{1}{n} \sum_{i=1}^n \mathcal{L}_{H, \beta}(\mathbf{x}_i; \theta', \phi')$ and vice-versa.

Proof. See Appendix A. \square

We thus see that optimising for (5) leads to networks equivalent to those from optimising the β -VAE objective (2), up to scaling the encodings by a factor of $\sqrt{\beta}$.

Under the isotropic Gaussian prior setting, we further have the following result showing that the β -VAE objective is invariant to rotations of the latent space.

Theorem 2. *If $p_\theta(\mathbf{z}) = \mathcal{N}(\mathbf{z}; 0, \sigma I)$ and $q_\phi(\mathbf{z} | \mathbf{x}) = \mathcal{N}(\mathbf{z}; \mu_\phi(\mathbf{x}), S_\phi(\mathbf{x}))$, then for all rotation matrices R ,*

$$\mathcal{L}_\beta(\mathbf{x}; \theta, \phi) = \mathcal{L}_\beta(\mathbf{x}; \theta^\dagger(R), \phi^\dagger(R)) \quad (6)$$

where $\theta^\dagger(R)$ and $\phi^\dagger(R)$ are transformed networks such that

$$\begin{aligned} p_{\theta^\dagger}(\mathbf{x} | \mathbf{z}) &= p_\theta(\mathbf{x} | R^T \mathbf{z}), \\ q_{\phi^\dagger}(\mathbf{z} | \mathbf{x}) &= \mathcal{N}(\mathbf{z}; \mu_{\phi^\dagger}(\mathbf{x}), S_{\phi^\dagger}(\mathbf{x})), \\ \mu_{\phi^\dagger}(\mathbf{x}) &= R \mu_\phi(\mathbf{x}), \\ S_{\phi^\dagger}(\mathbf{x}) &= R S_\phi(\mathbf{x}) R^T. \end{aligned}$$

Proof. If $\mathbf{z} \sim q_\phi(\mathbf{z} | \mathbf{x})$ and $\mathbf{y} = R\mathbf{z}$ then, by Petersen et al. (§8.1.4 2008)), we have

$$\begin{aligned} \mathbf{y} &\sim \mathcal{N}(\mathbf{y}; R \mu_\phi(\mathbf{x}), R S_\phi(\mathbf{x}) R^T) \quad \text{and thus} \\ \mathbf{y} &\sim \mathcal{N}(\mathbf{y}; \mu_{\phi^\dagger}(\mathbf{x}), S_{\phi^\dagger}(\mathbf{x})). \end{aligned}$$

Consequently, the changes made by the transformed networks cancel to give the same reconstruction error as

$$\begin{aligned}\mathbb{E}_{q_\phi(\mathbf{z}|\mathbf{x})}[\log p_\theta(\mathbf{x}|\mathbf{z})] &= \mathbb{E}_{q_{\phi^\dagger}(\mathbf{z}|\mathbf{x})}[\log p_\theta(\mathbf{x}|R^T\mathbf{z})] \\ &= \mathbb{E}_{q_{\phi^\dagger}(\mathbf{z}|\mathbf{x})}[\log p_{\theta^\dagger}(\mathbf{x}|\mathbf{z})].\end{aligned}$$

Furthermore, the KL divergence between $q_\phi(\mathbf{z}|\mathbf{x})$ and $p_\theta(\mathbf{z})$ is invariant to rotation, because of the rotational symmetry of the latter, such that $\text{KL}(q_\phi(\mathbf{z}|\mathbf{x})\|p(\mathbf{z})) = \text{KL}(q_{\phi^\dagger}(\mathbf{z}|\mathbf{x})\|p(\mathbf{z}))$. The result now follows from noting that the two terms of the β -VAE are equal under rotation. \square

This dispels the conjecture that the β -VAE objective encourages latent variables to take on meaningful representations (Burgess et al., 2018; Higgins et al., 2016), when using the standard choice of an isotropic Gaussian prior. In fact, it encourages latent representations which match true generative factors no more than it encourages them to match *any arbitrary rotation* of these factors, with such rotations capable of exhibiting strong correlations between latents. This view is further supported by our empirical results (see Figure 2), calculated over a large number of independently trained networks, where we did not observe any gains in disentanglement (using the metric from Kim and Mnih (2018)) from increasing $\beta > 1$ with an isotropic Gaussian prior trained on the *2D Shapes* dataset (Matthey et al., 2017). It may also go some way to explaining the extremely high levels of variation we found in the disentanglement-metric scores between different random seeds at train time. We note that an equivalent result to Theorem 2 was recently independently derived by Rolinek et al. (2018).

5. An Objective for Enforcing Decomposition

Given the characterisation set out above, we now develop an objective that incorporates the effect of both factors (a) and (b). Our analysis of the β -VAE tells us that its objective allows direct control over the level of overlap, i.e. factor (a). To incorporate direct control over the regularisation (b) between the marginal posterior and the prior, we add a divergence term $\mathbb{D}(q_\phi(\mathbf{z}), p(\mathbf{z}))$, yielding

$$\begin{aligned}\mathcal{L}_{\alpha,\beta}(\mathbf{x}) &= \mathbb{E}_{q_\phi(\mathbf{z}|\mathbf{x})}[\log p_\theta(\mathbf{x}|\mathbf{z})] \\ &\quad - \beta \text{KL}(q_\phi(\mathbf{z}|\mathbf{x})\|p(\mathbf{z})) - \alpha \mathbb{D}(q_\phi(\mathbf{z}), p(\mathbf{z}))\end{aligned}\quad (7)$$

allowing control over how much factors (a) and (b) are enforced, through appropriate setting of β and α respectively.

Note that such an additional term has been previously considered by Kumar et al. (2017), with $\mathbb{D}(q_\phi(\mathbf{z}), p(\mathbf{z})) = \text{KL}(q_\phi(\mathbf{z})\|p(\mathbf{z}))$, although for the sake of tractability they rely instead on moment matching using covariances. There have also been a number of approaches that decompose the standard VAE objective in different ways (e.g. Dilokthanakul et al., 2019; Esmaeili et al., 2018; Hoffman and

Johnson, 2016) to expose $\text{KL}(q_\phi(\mathbf{z})\|p(\mathbf{z}))$ as a component, but, as we discuss in Appendix C, this can be difficult to compute correctly in practice, with common approaches leading to highly biased estimates whose practical behaviour is very different than the divergence they are estimating, unless vary large batch sizes are used.

Wasserstein Auto-Encoders (Tolstikhin et al., 2017) formulate an objective that includes a general divergence term between the prior and marginal posterior, which are instantiated using either maximum mean discrepancy (MMD) or a variational formulation of the Jensen-Shannon divergence (a.k.a GAN loss). However, we find that empirically, choosing the MMD’s kernel and numerically stabilising its U-statistics estimator to be tricky, and designing and learning a GAN to be cumbersome and unstable. Consequently, the problems of choosing an appropriate $\mathbb{D}(q_\phi(\mathbf{z}), p(\mathbf{z}))$ and generating reliable estimates for this choice are tightly coupled, with a general purpose solution remaining an important open problem; see further discussion in Appendix C.

6. Experiments

6.1. Prior for axis-aligned disentanglement

First, we show how subtle changes to the prior distribution can yield improvement in terms of a common notion of disentanglement (see §4 in Kim and Mnih, 2018), namely *independence*. The most common choice of prior, an isotropic Gaussian, $p_\theta(\mathbf{z}) = \mathcal{N}(\mathbf{z}; \mathbf{0}, \mathbf{I})$, has previously been justified by the correct assertion that the latents are independent under the prior (Higgins et al., 2016). However, an isotropic Gaussian is also *rotationally invariant* and so does not constrain the axes of the latent space to capture any meaning. Non-isotropic Gaussians or other factored distributions such as product of Student-t’s can help break that rotational invariance while preserving independence. Such priors should therefore be better suited for learning disentangled representations. We assess that hypothesis by training a β -VAE (i.e. (7) with $\alpha = 0$) on the *2D Shapes* dataset (Matthey et al., 2017).

Figure 2 demonstrates that notable improvements in disentanglement can be achieved by using non-isotropic priors: for a given reconstruction loss, implicitly fixed by β , non-isotropic Gaussian priors get better disentanglement scores, with improvement achieved when the prior variance is learnt. With a product of Student-t priors p_ν (noting $p_\nu(\mathbf{z}) \rightarrow \mathcal{N}(\mathbf{z}; \mathbf{0}, \mathbf{I})$ as $\nu \rightarrow \infty$), reducing ν only incurs a minor reconstruction penalty, for improved disentanglement. Interestingly, very low values of ν caused the disentanglement score to drop again (though still giving higher values than the Gaussian). We speculate that this may be related to the effect of heavy tails on the disentanglement metric itself, rather than being an objectively worse disentanglement.

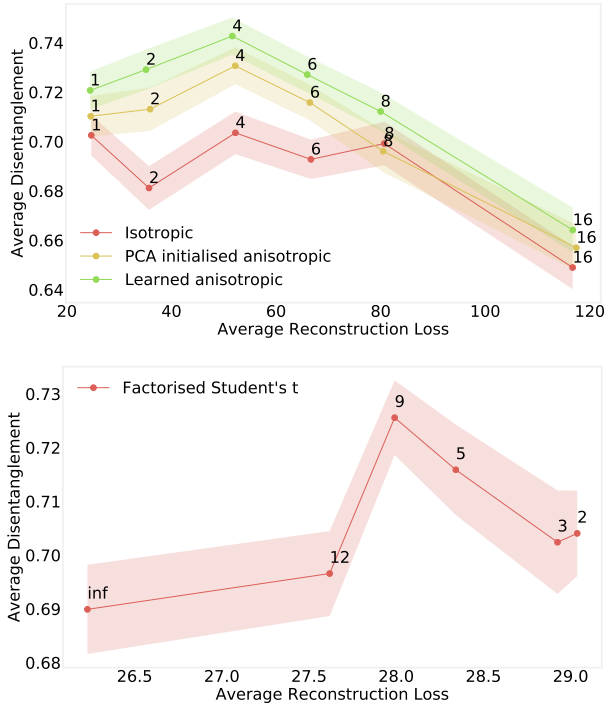


Figure 2. Reconstruction loss vs disentanglement (Kim and Mnih, 2018). Shaded areas represent 95% confidence intervals for estimated disentanglement, calculated using 100 separately trained networks. See Appendix B for details. [Top] Using an anisotropic Gaussian with diagonal covariance either learned, or fixed to principal-component values of the dataset. Point labels represent different values of β . [Bottom] Using $p_\nu(\mathbf{z}) = \prod_i \text{STUDENT-T}(z_i; \nu)$ for different ν with $\beta = 1$.

6.2. Clustered prior

We next consider an alternative decomposition one might wish to impose—*clustering* of the latent space. For this, we use the “pinwheels” dataset from (Johnson et al., 2016) and a mixture of four equally-weighted Gaussians as our prior. We then conduct an ablation study to observe the effect of varying α and β in $\mathcal{L}_{\alpha,\beta}(\mathbf{x})$ (as per (7)) on the learned representations, taking the divergence to be $\text{KL}(p(\mathbf{z})||q_\phi(\mathbf{z}))$ (see Appendix B for details). We see in Figure 3 that increasing β increases the level of overlap in $q_\phi(\mathbf{z})$, as a consequence of increasing the encoder variance for individual datapoints. When β is too large, the encoding of a datapoint loses meaning. Also, as a single datapoint encodes to a Gaussian distribution, $q_\phi(\mathbf{z}|\mathbf{x})$ is unable to match $p_\theta(\mathbf{z})$ exactly. Because $q_\phi(\mathbf{z}|\mathbf{x}) \rightarrow q_\phi(\mathbf{z})$ when $\beta \rightarrow \infty$, this in turn means that overly large values of β actually cause a mismatch between $q_\phi(\mathbf{z})$ and $p_\theta(\mathbf{z})$ (see top right of Figure 3). Increasing α , instead always improves the match between $q_\phi(\mathbf{z})$ and $p_\theta(\mathbf{z})$. Here, the finiteness of the dataset and the choice of divergence results in an increase in overlap with increasing α , but only up to the level required for a non-negligible overlap between the nearby datapoints: large values of α do not cause the encodings to collapse to a mode.

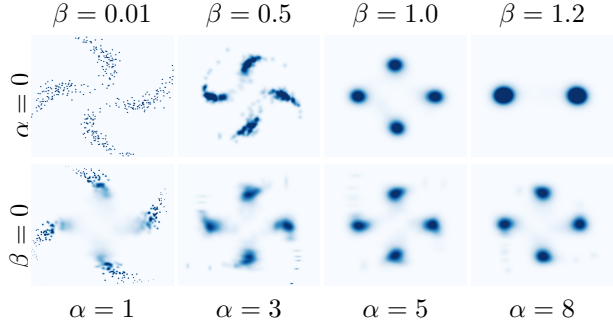


Figure 3. Density of aggregate posterior $q_\phi(\mathbf{z})$ with different α, β for spirals dataset with mixture of Gaussian prior.

6.3. Prior for sparsity

Finally, we consider a commonly desired decomposition—sparsity, which stipulates that only a small fraction of available factors are employed. That is, a *sparse representation* (Olshausen and Field, 1996) can be thought of as one where each embedding has a significant proportion of its dimensions *off*, i.e. close to 0. Sparsity has often been considered for feature-learning (Coates and Ng, 2011; Larochelle and Bengio, 2008) and employed in the probabilistic modelling literature (Lee et al., 2007; Ranzato et al., 2007). In this experiment, we measure sparsity through the *Hoyer* extrinsic metric (Hurley and Rickard, 2008), defined for $\mathbf{z} \in \mathbb{R}^d$ by

$$\text{Hoyer}(\mathbf{z}) = \frac{\sqrt{d} - \|\mathbf{z}\|_1 / \|\mathbf{z}\|_2}{\sqrt{d} - 1} \in [0, 1],$$

yielding 0 for a fully dense vector and 1 for a fully sparse vector. Common ways to achieve sparsity are through a specific penalty (e.g. l_1) or a careful choice of priors (peaked at 0). Concomitant with our overarching desire to encode requisite structure in the prior, we adopt the latter, constructing a sparse prior as $p(\mathbf{z}) = \prod_i (1 - \gamma) \mathcal{N}(z_i; 0, 1) + \gamma \mathcal{N}(z_i; 0, \sigma_0^2)$ with $\sigma_0^2 = 0.05$. This mixture distribution can be interpreted as a mixture of samples being either *off* or *on*, whose proportion is set by the weight parameter γ .

We use this prior to model the *CelebA* dataset (Liu et al., 2015) using the objective $\mathcal{L}_{\alpha,\beta}(\mathbf{x})$ (as per (7)), taking the divergence to be a MMD with *inverse multiquadratics* kernel (see Appendix B for details). Our ablation studies show Figure 4 (left) that substantial sparsity can be gained by replacing a Gaussian prior ($\gamma = 0$) by a sparse prior ($\gamma = 0.9$). It further shows substantial gains from the inclusion of the aggregate posterior regularization, with $\alpha = 0$ giving far low sparsity than $\alpha > 0$, when using our sparse prior. The use of our sparse prior does incur a small loss in reconstruction, as does increasing α , but both of these effects are very small compared to the losses from increasing β .

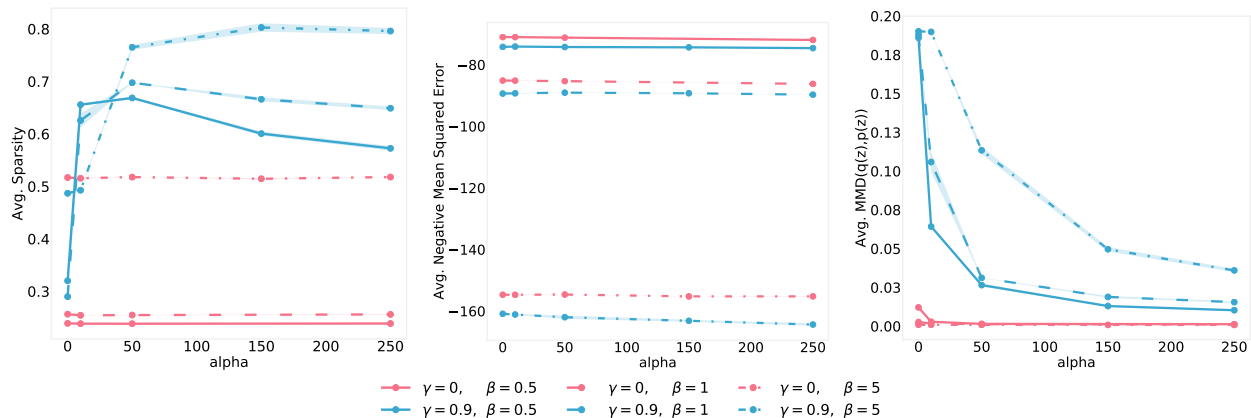


Figure 4. [Left] Sparsity vs regularisation strength α (c.f. (7)). [Center] Reconstruction loss vs α . [Right] Divergence (MMD) vs α . Note here that the different values of γ represent regularizations to different distributions, with regularization to a Gaussian (i.e. $\gamma = 0$) much easier to achieve than the sparse prior, hence the lower divergence. Shaded areas represent 95% confidence intervals calculated using 3 separately trained networks. See Appendix B for details.

7. Discussion

In this work, we explored and analysed the fundamental characteristics of learning disentangled representations, and showed how these can be generalized to a more general framework of *decomposition* (Lipton, 2016). We characterised the learning of decomposed latent representation with VAEs in terms of the control of two factors: i) overlap in the latent space between encodings of different datapoints, and ii) regularisation of the aggregate encoding distribution to the given prior, which encodes the structure one would wish for the latent space to have.

Connecting prior work on disentanglement to this framework, we analysed the β -VAE objective to show that its contribution to disentanglement is primarily through direct control of the level of overlap between encodings of the data, expressed by maximising the entropy of the encoding distribution. In the commonly encountered case of assuming an isotropic Gaussian prior and an independent Gaussian posterior, we showed that control of overlap is the *only* effect of the β -VAE. Motivated by this observation, we developed an alternate objective for the ELBO that allows control of the two factors of decomposability through an additional regularisation term. We then conducted empirical evaluations using this objective, targeting alternate forms of decompositions such as clustering and sparsity, and observed the effect of varying the extent of regularisation to the prior on the quality of the resulting clustering and sparseness of the learnt embeddings. The results indicate that we were successful in attaining those decompositions.

In very recently published work, (Locatello et al., 2018) question the plausibility of learning unsupervised disentangled representations with meaningful features, based on theoretical analyses showing an equivalence class of generative models, many members of which could be entangled. Though their analysis is sound, we posit a counterargu-

ment to their conclusions, based on *stochastic* nature of the encodings used during training. Namely, that this stochasticity means that they need not give rise to the same ELBO scores (an important exception is the rotational invariance for isotropic Gaussian priors). Essentially, the encoding noise forces nearby encodings to relate to similar datapoints, while standard choices for the likelihood distribution (e.g. assuming conditional independence) ensure that information is stored in the encodings, not just in the generative network. These restrictions mean that the ELBO prefers smooth representations and, provided the prior is not rotationally invariant, means that there no longer need be an class of different representations with the same ELBO; simpler representations are preferred to more complex ones.

The exact form of the encoding distribution is also important here. For example, imagine we restrict the encoder variance to be isotropic and then use a two dimensional prior where one latent dimension has much larger variance than the other. Here, it is possible to store more information in the prior dimension with higher variance (as we can spread points out more relative to the encoder variance). Consequently, that dimension is more likely to correspond to an important factor of the generative process than the other dimension. Of course this does not imply that this is a true factor of variation in the generative process, but neither is the meaning that can be attributed to each dimension completely arbitrary.

All the same, we agree with the general sentiment that an important area for future work is to assess when, and to what extent, one might expect learned representations to mimic the true generative process, and, critically, when it should not. For this reason, we actively avoid including any notion of a true generative process in our definition of decomposition, but note that, analogously to disentanglement, it permits such extension in scenarios where doing so can be shown to be appropriate.

References

- Alessandro Achille and Stefano Soatto. Emergence of invariance and disentanglement in deep representations. *Journal of Machine Learning Research*, 19(50), 2019.
- Alexander Alemi, Ben Poole, Ian Fischer, Joshua Dillon, Rif A Saurous, and Kevin Murphy. Fixing a broken elbo. In *International Conference on Machine Learning*, pages 159–168, 2018.
- Alexander A Alemi, Ian Fischer, Joshua V Dillon, and Kevin Murphy. Deep variational information bottleneck. In *International Conference on Learning Representations*, 2017.
- Abdul Fatir Ansari and Harold Soh. Hyperprior Induced Unsupervised Disentanglement of Latent Representations. *arXiv.org*, September 2018.
- Yoshua Bengio, Aaron Courville, and Pascal Vincent. Representation learning: A review and new perspectives. *IEEE Trans. Pattern Anal. Mach. Intell.*, 35(8):1798–1828, August 2013. ISSN 0162-8828.
- Diane Bouchacourt, Ryota Tomioka, and Sebastian Nowozin. Multi-level variational autoencoder: Learning disentangled representations from grouped observations. In *Proceedings of the Thirty-Second AAAI Conference on Artificial Intelligence, New Orleans, Louisiana, USA, February 2-7, 2018*, 2018.
- Christopher P. Burgess, Irina Higgins, Arka Pal, Loïc Matthey, Nick Watters, Guillaume Desjardins, and Alexander Lerchner. Understanding disentangling in β -vae. *CoRR*, abs/1804.03599, 2018.
- Tian Qi Chen, Xuechen Li, Roger Grosse, and David Duvenaud. Isolating sources of disentanglement in variational autoencoders. *arXiv preprint arXiv:1802.04942*, 2018.
- Xi Chen, Yan Duan, Rein Houthoofd, John Schulman, Ilya Sutskever, and Pieter Abbeel. Infogan: Interpretable representation learning by information maximizing generative adversarial nets. In *Advances in neural information processing systems*, pages 2172–2180, 2016a.
- Xi Chen, Diederik P Kingma, Tim Salimans, Yan Duan, Prafulla Dhariwal, John Schulman, Ilya Sutskever, and Pieter Abbeel. Variational Lossy Autoencoder. *arXiv.org*, November 2016b.
- Brian Cheung, Jesse A Livezey, Arjun K Bansal, and Bruno A Olshausen. Discovering hidden factors of variation in deep networks. *arXiv preprint arXiv:1412.6583*, 2014.
- Adam Coates and Andrew Y. Ng. The importance of encoding versus training with sparse coding and vector quantization. In Lise Getoor and Tobias Scheffer, editors, *ICML*, pages 921–928. Omnipress, 2011.
- Nat Dilokthanakul, Nick Pawlowski, and Murray Shanahan. Explicit information placement on latent variables using auxiliary generative modelling task, 2019. URL <https://openreview.net/forum?id=H11-SjA5t7>.
- Justin Domke and Daniel Sheldon. Importance weighting and variational inference. *arXiv preprint arXiv:1808.09034*, 2018.
- Cian Eastwood and Christopher K. I. Williams. A framework for the quantitative evaluation of disentangled representations. In *International Conference on Learning Representations*, 2018.
- Babak Esmaeili, Hao Wu, Sarthak Jain, N Siddharth, Brooks Paige, and Jan-Willem van de Meent. Hierarchical Disentangled Representations. *arXiv.org*, April 2018.
- Irina Higgins, Loic Matthey, Arka Pal, Christopher Burgess, Xavier Glorot, Matthew Botvinick, Shakir Mohamed, and Alexander Lerchner. beta-VAE: Learning basic visual concepts with a constrained variational framework. In *Proceedings of the International Conference on Learning Representations (ICLR)*, 2016.
- Irina Higgins, David Amos, David Pfau, Sebastien Racaniere, Loic Matthey, Danilo Rezende, and Alexander Lerchner. Towards a definition of disentangled representations. *arXiv preprint arXiv:1812.02230*, 2018.
- R Devon Hjelm, Alex Fedorov, Samuel Lavoie-Marchildon, Karan Grewal, Adam Trischler, and Yoshua Bengio. Learning deep representations by mutual information estimation and maximization. *arXiv preprint arXiv:1808.06670*, 2018.
- Matthew D Hoffman and Matthew J Johnson. ELBO surgery: yet another way to carve up the variational evidence lower bound. In *Workshop on Advances in Approximate Bayesian Inference, NIPS*, pages 1–4, 2016.
- Matthew D Hoffman, Carlos Riquelme, and Matthew J Johnson. The β -VAE’s Implicit Prior. In *Workshop on Bayesian Deep Learning, NIPS*, pages 1–5, 2017.
- Niall P. Hurley and Scott T. Rickard. Comparing measures of sparsity. *IEEE Transactions on Information Theory*, 55:4723–4741, 2008.
- Aapo Hyvärinen and Erkki Oja. Independent component analysis: algorithms and applications. *Neural networks*, 13(4-5):411–430, 2000.

- Matthew J Johnson, David Duvenaud, Alexander B Wiltschko, Sandeep R Datta, and Ryan P Adams. Composing graphical models with neural networks for structured representations and fast inference. *arXiv.org*, March 2016.
- Hyunjik Kim and Andriy Mnih. Disentangling by factorising. *CoRR*, abs/1802.05983, 2018.
- Diederik P Kingma and Jimmy Ba. Adam: A Method for Stochastic Optimization. *arXiv.org*, December 2014.
- Diederik P. Kingma and Max Welling. Auto-encoding variational bayes. In *International Conference on Learning Representations*, 2014.
- Diederik P Kingma, Shakir Mohamed, Danilo Jimenez Rezende, and Max Welling. Semi-supervised learning with deep generative models. In *Advances in Neural Information Processing Systems*, 2014.
- Abhishek Kumar, Prasanna Sattigeri, and Avinash Balakrishnan. Variational Inference of Disentangled Latent Concepts from Unlabeled Observations. *arXiv.org*, November 2017.
- Hugo Larochelle and Yoshua Bengio. Classification using discriminative restricted boltzmann machines. In *Proceedings of the 25th International Conference on Machine Learning, ICML '08*, pages 536–543, New York, NY, USA, 2008. ACM. ISBN 978-1-60558-205-4.
- Honglak Lee, Alexis Battle, Rajat Raina, and Andrew Y. Ng. Efficient sparse coding algorithms. In B. Schölkopf, J. C. Platt, and T. Hoffman, editors, *Advances in Neural Information Processing Systems 19*, pages 801–808. MIT Press, 2007.
- Zachary C Lipton. The mythos of model interpretability. *arXiv preprint arXiv:1606.03490*, 2016.
- Ziwei Liu, Ping Luo, Xiaogang Wang, and Xiaoou Tang. Deep learning face attributes in the wild. In *Proceedings of International Conference on Computer Vision (ICCV)*, December 2015.
- Francesco Locatello, Stefan Bauer, Mario Lucic, Sylvain Gelly, Bernhard Schölkopf, and Olivier Bachem. Challenging common assumptions in the unsupervised learning of disentangled representations. *arXiv preprint arXiv:1811.12359*, 2018.
- Chris J Maddison, John Lawson, George Tucker, Nicolas Heess, Mohammad Norouzi, Andriy Mnih, Arnaud Doucet, and Yee Teh. Filtering variational objectives. In *Advances in Neural Information Processing Systems*, pages 6573–6583, 2017.
- Alireza Makhzani, Jonathon Shlens, Navdeep Jaitly, Ian Goodfellow, and Brendan Frey. Adversarial autoencoders. *arXiv preprint arXiv:1511.05644*, 2015.
- Michael F Mathieu, Junbo Jake Zhao, Junbo Zhao, Aditya Ramesh, Pablo Sprechmann, and Yann LeCun. Disentangling factors of variation in deep representation using adversarial training. In *Advances in Neural Information Processing Systems*, pages 5040–5048, 2016.
- Loic Matthey, Irina Higgins, Demis Hassabis, and Alexander Lerchner. dsprites: Disentanglement testing sprites dataset. <https://github.com/deepmind/dsprites-dataset/>, 2017.
- B. Olshausen and D. Field. Emergence of simple-cell receptive field properties by learning a sparse code for natural images. *Nature*, 381:607–609, 1996.
- Kaare Brandt Petersen, Michael Syskind Pedersen, et al. The matrix cookbook. *Technical University of Denmark*, 7(15):510, 2008.
- Mary Phuong, Max Welling, Nate Kushman, Ryota Tomioka, and Sebastian Nowozin. The mutual autoencoder: Controlling information in latent code representations, 2018. URL <https://openreview.net/forum?id=HkbnWqxqCZ>.
- Alec Radford, Luke Metz, and Soumith Chintala. Unsupervised representation learning with deep convolutional generative adversarial networks. *CoRR*, abs/1511.06434, 2015.
- Tom Rainforth, Robert Cornish, Hongseok Yang, Andrew Warrington, and Frank Wood. On nesting monte carlo estimators. In *International Conference on Machine Learning*, pages 4264–4273, 2018a.
- Tom Rainforth, Adam R. Kosiorek, Tuan Anh Le, Chris J. Maddison, Maximilian Igl, Frank Wood, and Yee Whye Teh. Tighter variational bounds are not necessarily better. *International Conference on Machine Learning (ICML)*, 2018b.
- Marc Ranzato, Christopher Poultney, Sumit Chopra, and Yann L. Cun. Efficient learning of sparse representations with an energy-based model. In *Advances in Neural Information Processing Systems 19*, pages 1137–1144. MIT Press, 2007.
- Sashank J. Reddi, Satyen Kale, and Sanjiv Kumar. On the convergence of adam and beyond. In *International Conference on Learning Representations*, 2018.
- Scott Reed, Kihyuk Sohn, Yuting Zhang, and Honglak Lee. Learning to disentangle factors of variation with manifold interaction. In *International Conference on Machine Learning*, pages 1431–1439, 2014.

- Danilo Jimenez Rezende, Shakir Mohamed, and Daan Wierstra. Stochastic backpropagation and approximate inference in deep generative models. *arXiv preprint arXiv:1401.4082*, 2014.
- Michal Rolínek, Dominik Zietlow, and Georg Martius. Variational Autoencoders Pursue PCA Directions (by Accident). *arXiv preprint arXiv:1812.06775*, 2018.
- Jürgen Schmidhuber. Learning factorial codes by predictability minimization. *Neural Computation*, 4(6):863–879, 1992.
- N. Siddharth, T Brooks Paige, Jan-Willem Van de Meent, Alban Desmaison, Noah Goodman, Pushmeet Kohli, Frank Wood, and Philip Torr. Learning disentangled representations with semi-supervised deep generative models. In *Advances in Neural Information Processing Systems*, pages 5925–5935, 2017.
- Ilya Tolstikhin, Olivier Bousquet, Sylvain Gelly, and Bernhard Schölkopf. Wasserstein Auto-Encoders. *arXiv.org*, November 2017.
- Jiacheng Xu and Greg Durrett. Spherical Latent Spaces for Stable Variational Autoencoders. *arXiv.org*, August 2018.
- Howard Hua Yang and Shun-ichi Amari. Adaptive online learning algorithms for blind separation: maximum entropy and minimum mutual information. *Neural computation*, 9(7):1457–1482, 1997.
- Shengjia Zhao, Jiaming Song, and Stefano Ermon. Infovae: Information maximizing variational autoencoders. *CoRR*, abs/1706.02262, 2017. URL <http://arxiv.org/abs/1706.02262>.

Appendix: Disentangling Disentanglement for Variational Auto-Encoders

A. Proofs for Disentangling the β -VAE

Corollary 1. *If $p_\theta(\mathbf{z}) = \mathcal{N}(\mathbf{z}; 0, \Sigma)$ and $q_\phi(\mathbf{z} | \mathbf{x}) = \mathcal{N}(\mathbf{z}; \mu_\phi(\mathbf{x}), S_\phi(\mathbf{x}))$, then,*

$$\mathcal{L}_\beta(\mathbf{x}; \theta, \phi) = \mathcal{L}(\mathbf{x}; \theta', \phi') + \frac{(\beta - 1)}{2} \log |S_{\phi'}(\mathbf{x})| + c \quad (4)$$

where θ' and ϕ' represent rescaled networks such that

$$\begin{aligned} p_{\theta'}(\mathbf{x} | \mathbf{z}) &= p_\theta(\mathbf{x} | \mathbf{z} / \sqrt{\beta}), \\ q_{\phi'}(\mathbf{z} | \mathbf{x}) &= \mathcal{N}(\mathbf{z}; \mu_{\phi'}(\mathbf{x}), S_{\phi'}(\mathbf{x})), \\ \mu_{\phi'}(\mathbf{x}) &= \sqrt{\beta} \mu_\phi(\mathbf{x}), \\ S_{\phi'}(\mathbf{x}) &= \beta S_\phi(\mathbf{x}), \end{aligned}$$

and $c \triangleq \frac{D(\beta-1)}{2} \left(1 + \log \frac{2\pi}{\beta}\right) + \log F_\beta$ is a constant, with D denoting the dimensionality of \mathbf{z} .

Proof. We start by noting that

$$\begin{aligned} \pi_{\theta, \beta}(\mathbf{x}) &= \mathbb{E}_{f_\beta(\mathbf{z})} [p_\theta(\mathbf{x} | \mathbf{z})] = \mathbb{E}_{p_\theta(\mathbf{z})} [p_\theta(\mathbf{x} | \mathbf{z} / \sqrt{\beta})] \\ &= \mathbb{E}_{p_\theta(\mathbf{z})} [p_{\theta'}(\mathbf{x} | \mathbf{z})] = p_{\theta'}(\mathbf{x}) \end{aligned}$$

Now considering an alternate form of $\mathcal{L}(\mathbf{x}; \pi_{\theta, \beta}, q_\phi)$ in (3),

$$\begin{aligned} \mathcal{L}(\mathbf{x}; \pi_{\theta, \beta}, q_\phi) &= \log \pi_{\theta, \beta}(\mathbf{x}) - \text{KL}(q_\phi(\mathbf{z} | \mathbf{x}) \| \pi_{\theta, \beta}(\mathbf{z} | \mathbf{x})) \\ &= \log p_{\theta'}(\mathbf{x}) - \mathbb{E}_{q_\phi(\mathbf{z} | \mathbf{x})} \left[\log \left(\frac{q_\phi(\mathbf{z} | \mathbf{x}) p_{\theta'}(\mathbf{x})}{p_\theta(\mathbf{x} | \mathbf{z}) f_\beta(\mathbf{z})} \right) \right] \\ &= \log p_{\theta'}(\mathbf{x}) \\ &\quad - \mathbb{E}_{q_{\phi'}(\mathbf{z} | \mathbf{x})} \left[\log \left(\frac{q_\phi(\mathbf{z} / \sqrt{\beta} | \mathbf{x}) p_{\theta'}(\mathbf{x})}{p_\theta(\mathbf{x} | \mathbf{z} / \sqrt{\beta}) f_\beta(\mathbf{z} / \sqrt{\beta})} \right) \right]. \quad (8) \end{aligned}$$

We first simplify $f_\beta(\mathbf{z} / \sqrt{\beta})$ as

$$\begin{aligned} f_\beta(\mathbf{z} / \sqrt{\beta}) &= \frac{1}{\sqrt{2\pi}^{|\Sigma|/\beta}} \exp\left(-\frac{1}{2} \mathbf{z}^T \Sigma^{-1} \mathbf{z}\right) \\ &= p(\mathbf{z}) \beta^{(D/2)}. \end{aligned}$$

Further, denoting $\mathbf{z}_\dagger = \mathbf{z} - \sqrt{\beta} \mu_{\phi'}(\mathbf{x})$, and $\mathbf{z}_\ddagger = \mathbf{z}_\dagger / \sqrt{\beta} = \mathbf{z} / \sqrt{\beta} - \mu_{\phi'}(\mathbf{x})$, we have

$$\begin{aligned} q_{\phi'}(\mathbf{z} | \mathbf{x}) &= \frac{1}{\sqrt{2\pi}^{|\Sigma_\phi(\mathbf{x})|} \beta} \exp\left(-\frac{1}{2\beta} \mathbf{z}_\dagger^T S_\phi(\mathbf{x})^{-1} \mathbf{z}_\dagger\right), \\ q_\phi\left(\frac{\mathbf{z}}{\sqrt{\beta}} | \mathbf{x}\right) &= \frac{1}{\sqrt{2\pi}^{|\Sigma_\phi(\mathbf{x})|}} \exp\left(-\frac{1}{2} \mathbf{z}_\ddagger^T S_\phi(\mathbf{x})^{-1} \mathbf{z}_\ddagger\right) \\ \text{giving } q_\phi\left(\mathbf{z} / \sqrt{\beta} | \mathbf{x}\right) &= q_{\phi'}(\mathbf{z} | \mathbf{x}) \beta^{(D/2)}. \end{aligned}$$

Plugging these back in to (8) while remembering $p_\theta(\mathbf{x} | \mathbf{z} / \sqrt{\beta}) = p_{\theta'}(\mathbf{x} | \mathbf{z})$, we have

$$\begin{aligned} \mathcal{L}(\mathbf{x}; \pi_{\theta, \beta}, q_\phi) &= \log p_{\theta'}(\mathbf{x}) - \mathbb{E}_{q_{\phi'}(\mathbf{z} | \mathbf{x})} \left[\log \left(\frac{q_{\phi'}(\mathbf{z} | \mathbf{x}) p_{\theta'}(\mathbf{x})}{p_{\theta'}(\mathbf{x} | \mathbf{z}) p(\mathbf{z})} \right) \right] \\ &= \mathcal{L}(\mathbf{x}; \theta, \phi), \end{aligned}$$

showing that the ELBOs for the two setups are the same. For the entropy term, we note that

$$\begin{aligned} H_{q_\phi} &= \frac{D}{2} (1 + \log 2\pi) + \frac{1}{2} \log |S_\phi(\mathbf{x})| \\ &= \frac{D}{2} \left(1 + \log \frac{2\pi}{\beta}\right) + \frac{1}{2} \log |S_{\phi'}(\mathbf{x})|. \end{aligned}$$

Finally substituting for H_{q_ϕ} and $\mathcal{L}(\mathbf{x}; \pi_{\theta, \beta}, q_\phi)$ in (3) gives the desired result. \square

Corollary 2. *Let $[\theta', \phi'] = g_\beta([\theta, \phi])$ represent the transformation required to produce the rescaled networks in Corollary 1. If $0 < |\det \nabla_{\theta, \phi} g([\theta, \phi])| < \infty \forall [\theta, \phi]$, then*

$$\nabla_{\theta, \phi} \mathcal{L}_\beta(\mathbf{x}; \theta, \phi) = \mathbf{0} \Leftrightarrow \nabla_{\theta', \phi'} \mathcal{L}_{H, \beta}(\mathbf{x}; \theta', \phi') = \mathbf{0}.$$

Thus $[\theta^*, \phi^*]$ being a stationary point of $\frac{1}{n} \sum_{i=1}^n \mathcal{L}_\beta(\mathbf{x}_i; \theta, \phi)$ indicates that $g_\beta([\theta^*, \phi^*])$ is a stationary point of $\frac{1}{n} \sum_{i=1}^n \mathcal{L}_{H, \beta}(\mathbf{x}_i; \theta', \phi')$ and vice-versa.

Proof. Starting from Corollary 1 we have that

$$\begin{aligned} \nabla_{\theta, \phi} \mathcal{L}_\beta(\mathbf{x}; \theta, \phi) &= \nabla_{\theta, \phi} \mathcal{L}_{H, \beta}(\mathbf{x}; \theta', \phi') \\ &= (\nabla_{\theta, \phi} g_\beta([\theta, \phi])) \nabla_{\theta', \phi'} \mathcal{L}_{H, \beta}(\mathbf{x}; \theta', \phi'), \end{aligned}$$

so $\nabla_{\theta', \phi'} \mathcal{L}_{H, \beta}(\mathbf{x}; \theta', \phi') = \mathbf{0} \implies \nabla_{\theta, \phi} \mathcal{L}_\beta(\mathbf{x}; \theta, \phi) = \mathbf{0}$ given our assumption that $|\det \nabla_{\theta, \phi} g([\theta, \phi])| < \infty \forall [\theta, \phi]$. Further, as $0 < |\det \nabla_{\theta, \phi} g([\theta, \phi])| \forall [\theta, \phi]$, $(\nabla_{\theta, \phi} g_\beta([\theta, \phi]))^{-1}$ exists and has a finite determinant, so $\nabla_{\theta, \phi} \mathcal{L}_\beta(\mathbf{x}; \theta, \phi) = \mathbf{0}$ also implies $\nabla_{\theta', \phi'} \mathcal{L}_{H, \beta}(\mathbf{x}; \theta', \phi') = \mathbf{0}$. \square

B. Experimental Details

Disentanglement - 2d-shapes: The experiments from Section 6 on the impact of the prior in terms disentanglement are conducted on the **2D Shapes** (Matthey et al., 2017) dataset, comprising of 737,280 binary 64 x 64 images of 2D shapes with ground truth factors [number of values]: shape[3], scale[6], orientation[40], x-position[32], y-position[32]. We use a convolutional neural network for the encoder and a deconvolutional neural network for the decoder, whose architectures are described in Table 1a. We use $[0, 1]$ normalised data as targets for the mean of a Bernoulli

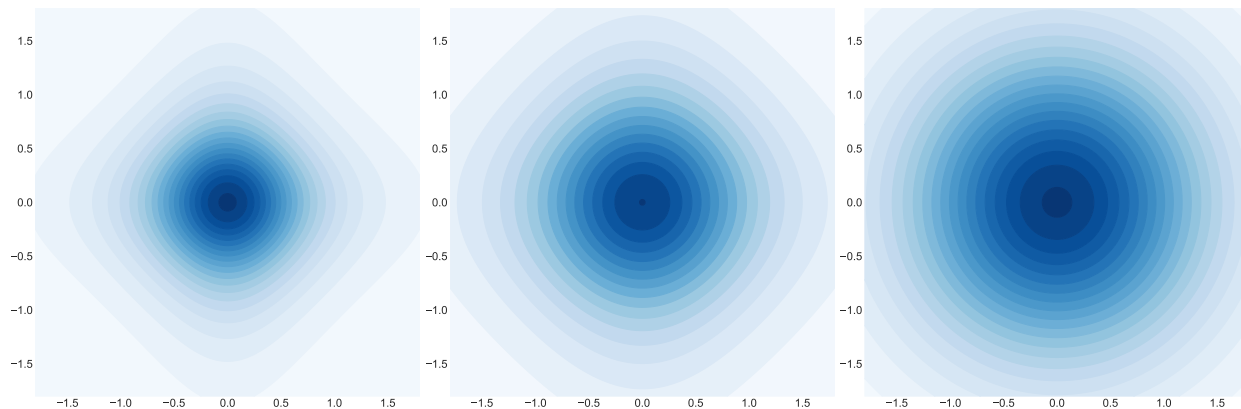


Figure 5. Probability density function for 2-dimensional factored Student-t distributions p_ν with degree of freedom $\nu = \{3, 5, 100\}$ (left to right). Note that $p_\nu(\mathbf{z}) \rightarrow \mathcal{N}(\mathbf{z}; \mathbf{0}, \mathbf{I})$ as $\nu \rightarrow \infty$.

Encoder	Decoder
Input 64 x 64 binary image	Input $\in \mathbb{R}^{10}$
4x4 conv. 32 stride 2 & ReLU	FC. 128 ReLU
4x4 conv. 32 stride 2 & ReLU	FC. 4x4 x 64 ReLU
4x4 conv. 64 stride 2 & ReLU	4x4 upconv. 64 stride 2 & ReLU
4x4 conv. 64 stride 2 & ReLU	4x4 upconv. 64 stride 2 & ReLU
FC. 128	4x4 upconv. 32 stride 2 & ReLU
FC. 2x10	4x4 upconv. 1. stride 2

(a) 2D-shapes dataset.

Encoder	Decoder
Input $\in \mathbb{R}^2$	Input $\in \mathbb{R}^2$
FC. 100. & ReLU	FC. 100 & ReLU
FC. 2x2	FC. 2x2

(b) Pinwheel dataset.

Encoder
Input 64 x 64 x 3 channels image
4x4 conv. 32 stride 2 & BatchNorm2d & LeakyReLU(.2)
4x4 conv. 64 stride 2 & BatchNorm2d & LeakyReLU(.2)
4x4 conv. 128 stride 2 & BatchNorm2d & LeakyReLU(.2)
4x4 conv. 256 stride 2 & BatchNorm2d & LeakyReLU(.2)
4x4 conv. 50, 4x4 conv. 50
Decoder
Input $\in \mathbb{R}^{50}$
4x4 upconv. 256 stride 1 & BatchNorm2d & ReLU
4x4 upconv. 128 stride 2 & BatchNorm2d & ReLU
4x4 upconv. 64 stride 2 & BatchNorm2d & ReLU
4x4 upconv. 32 stride 2 & BatchNorm2d & ReLU
4x4 upconv. 3 stride 2

(c) CelebA dataset.

Table 1. Encoder and decoder architectures.

distribution, using negative cross-entropy for $\log p(\mathbf{x}|\mathbf{z})$. We rely on the Adam optimiser (Kingma and Ba, 2014; Reddi et al., 2018) with learning rate $1e^{-4}$, $\beta_1 = 0.9$, $\beta_2 = 0.999$, to optimise the β -VAE objective from (3).

For $p_\theta(\mathbf{z}) = \mathcal{N}(\mathbf{z}; \mathbf{0}, \text{diag}(\sigma))$, experiments were run with a batch size of 64 and for 20 epochs. For $p_\theta(\mathbf{z}) =$

$\prod_i \text{STUDENT-T}(z_i; \nu)$, experiments were run with a batch size of 256 and for 40 epochs. In Figure 2, the *PCA initialised anisotropic* prior is initialised so that its standard deviations are set to be the first D singular values of the data. These are then mapped through a softmax function to ensure that the β regularisation coefficient is not implicitly scaled compared to the isotropic case. For the *learned anisotropic* priors, standard deviations are first initialised as just described, and then learned along the model through a log-variance parametrisation.

We rely on the metric presented in §4 and Appendix B of Kim and Mnih (2018) as a measure of axis-alignment of the latent encodings with respect to the true (known) generative factors. Confidence intervals in Figure 2 were computed via the assumption of normally distributed samples with unknown mean and variance, with 100 runs of each model.

Clustering - Pinwheel We generated spiral cluster data¹, with $n = 400$ observations, clustered in 4 spirals, with radial and tangential standard deviations respectively of 0.1 and 0.3, and a rate of 0.25. We use fully-connected neural networks for both the encoder and decoder, whose architectures are described in Table 1b. We minimise the objective from (7), with \mathbb{D} chosen to be the inclusive KL, with $q_\phi(\mathbf{z})$ approximated by the aggregate encoding of data

$$\begin{aligned}
 \mathbb{D}(q_\phi(\mathbf{z}), p(\mathbf{z})) &= \text{KL}(p(\mathbf{z}) || q_\phi(\mathbf{z})) \\
 &= \mathbb{E}_{p(\mathbf{z})} [\log(p(\mathbf{z})) - \log(\mathbb{E}_{p_{\mathcal{D}}(\mathbf{x})} [q_\phi(\mathbf{z} | \mathbf{x})])] \\
 &\approx \sum_{j=1}^B \left(\log p(\mathbf{z}_j) - \log \left(\sum_{i=1}^n q_\phi(\mathbf{z}_j | \mathbf{x}_i) \right) \right)
 \end{aligned}$$

with $\mathbf{z}_j \sim p(\mathbf{z})$. A Gaussian likelihood is used for the encoder. We trained the model for 500 epochs using the

¹<http://hips.seas.harvard.edu/content/synthetic-pinwheel-data-matlab>.



Figure 6. PDF of Gaussian mixture model prior $p(\mathbf{z})$, as per (9).

Adam optimiser (Kingma and Ba, 2014; Reddi et al., 2018), with $\beta_1 = 0.9$ and $\beta_2 = 0.999$ and a learning rate of $1e^{-3}$. The batch size is set to $B = n$.

The mixture of Gaussian prior (c.f. Figure 6) is defined as

$$p(\mathbf{z}) = \sum_{c=1}^C \pi_c \mathcal{N}(\mathbf{z} | \boldsymbol{\mu}_c, \boldsymbol{\Sigma}_c) = \sum_{c=1}^C \pi_c \prod_{d=1}^D \mathcal{N}(z^d | \mu_c^d, \sigma_c^d) \quad (9)$$

with $D = 2$, $C = 4$, $\boldsymbol{\Sigma}_c = .03I_D$, $\pi_c = 1/C$ & $\mu_c^d \in \{0, 1\}$.

Sparsity - CelebA The experiments from Section 6 on the latent representation’s sparsity are conducted on the cropped version of the **CelebA** (Liu et al., 2015) dataset, comprising of 202, 599 RGB 64 x 64 x 3 images of celebrity faces.

To enforce sparsity, we rely on a prior defined as factored univariate mixture of a standard and low variance normal distributions:

$$p(z) = \prod_i (1 - \gamma) \mathcal{N}(z_i; 0, 1) + \gamma \mathcal{N}(z_i; 0, \sigma_0^2),$$

with $\sigma_0 = 5e - 2$. The weight γ of the low-variance component, indicates how likely samples are to come from that component, hence to be *off*.

We minimise the objective from (7), with \mathbb{D} chosen to be a MMD with *inverse multiquadratics* kernel $k(\mathbf{x}, \mathbf{y}) = C / (C + \|\mathbf{x} - \mathbf{y}\|_2)$ as in (Tolstikhin et al., 2017).

We use a convolutional neural network for the encoder and a deconvolutional neural network for the decoder, whose architectures come from the DCGAN model (Radford et al., 2015) and are described in Table 1c. We rely on the Adam optimiser with learning rate $2e^{-4}$, $\beta_1 = 0.5$, $\beta_2 = 0.999$. The model is then trained (on the training set) for 60 epochs with a batch-size of 256.

As an extrinsic measure of *sparsity*, we use the *Hoyer* metric (Hurley and Rickard, 2008), defined for $\mathbf{z} \in \mathbb{R}^d$ by

$$\text{Hoyer}(\mathbf{z}) = \frac{\sqrt{d} - \frac{\|\mathbf{z}\|_1}{\|\mathbf{z}\|_2}}{\sqrt{d} - 1} \in [0, 1]$$

Hence $\text{Hoyer}(\mathbf{z}) = 0$ for a *dense* vector and $\text{Hoyer}(\mathbf{z}) = 1$ for a *sparse* vector. We then compute the average Hoyer metric over the dataset embeddings: $\text{Hoyer}(\mathbf{Z}) = \frac{1}{N} \sum_{i=1}^N \text{Hoyer}(\mathbf{z}_i)$.

C. Posterior regularisation

The aggregate posterior regulariser $\mathbb{D}(q(\mathbf{z}), p(\mathbf{z}))$ is a little more subtle to analyse than the entropy regulariser as it involves both the choice of divergence and potential difficulties in estimating that divergence. One possible choice is the exclusive Kullback-Leibler divergence $\text{KL}(q(\mathbf{z}) \parallel p(\mathbf{z}))$, as previously used (without additional entropy regularisation) by (Dilokthanakul et al., 2019; Esmaeili et al., 2018), but also implicitly by (Chen et al., 2018; Kim and Mnih, 2018), through the use of a total correlation (TC) term. We now highlight a shortfall with this choice of divergence due to difficulties in its empirical estimation.

In short, the approaches used to estimate the $\mathbb{H}[q(\mathbf{z})]$ (noting that $\text{KL}(q(\mathbf{z}) \parallel p(\mathbf{z})) = -\mathbb{H}[q(\mathbf{z})] - \mathbb{E}_{q(\mathbf{z})}[\log p(\mathbf{z})]$, where the latter term can be estimated reliably by a simple Monte Carlo estimate) can exhibit very large biases unless very large batch sizes are used, resulting in quite different effects from what was intended. In fact, our results suggest they will exhibit behaviour similar to the β -VAE if the batch size is too small. These biases arise from the effects of nesting estimators (Rainforth et al., 2018a), where the variance in the nested (inner) estimator for $q(\mathbf{z})$ induces a bias in the overall estimator. Specifically, for any random variable \hat{Z} ,

$$\mathbb{E}[\log(\hat{Z})] = \log(\mathbb{E}[\hat{Z}]) - \frac{\text{Var}[\hat{Z}]}{2\mathbb{E}[\hat{Z}]^2} + O(\varepsilon)$$

where $O(\varepsilon)$ represents higher-order moments that get dominated asymptotically if \hat{Z} is a Monte-Carlo estimator (see Proposition 1c in Maddison et al. (2017), Theorem 1 in Rainforth et al. (2018b), or Theorem 3 in Domke and Sheldon (2018)). In this setting, $\hat{Z} = \hat{q}(\mathbf{z})$ is the estimate used for $q(\mathbf{z})$. We thus see that if the variance of $\hat{q}(\mathbf{z})$ is large, this will induce a significant bias in our KL estimator.

To make things precise, we consider the estimator used for $\mathbb{H}[q(\mathbf{z})]$ in Chen et al. (2018); Dilokthanakul et al. (2019); Esmaeili et al. (2018)

$$\mathbb{H}[q(\mathbf{z})] \approx \hat{\mathbb{H}} \triangleq -\frac{1}{B} \sum_{b=1}^B \log \hat{q}(\mathbf{z}_b), \quad \text{where} \quad (10a)$$

$$\hat{q}(\mathbf{z}_b) = \frac{q_\phi(\mathbf{z}_b | \mathbf{x}_b)}{n} + \frac{n-1}{n(B-1)} \sum_{b' \neq b} q_\phi(\mathbf{z}_b | \mathbf{x}'_{b'}), \quad (10b)$$

$\mathbf{z}_b \sim q_\phi(\mathbf{z} | \mathbf{x}_b)$, and $\{\mathbf{x}_1, \dots, \mathbf{x}_B\}$ is the mini-batch of data used for the current iteration for dataset size n . Esmaeili et al. (2018) correctly show that $\mathbb{E}[\hat{q}(\mathbf{z}_b)] = \bar{q}(\mathbf{z}_b)$, with the first term of (10b) comprising an exact term in $\bar{q}(\mathbf{z}_b)$ and the second term of (10b) being an unbiased Monte-Carlo estimate for the remaining terms in $\bar{q}(\mathbf{z}_b)$.

To examine the practical behaviour of this estimator when $B \ll n$, we first note that the second term of (10b) is, in practice, usually very small and dominated by the first term.

This is borne out empirically in our own experiments, and also noted in [Kim and Mnih \(2018\)](#). To see why this is the case, consider that given encodings of two independent data points, it is highly unlikely that the two encoding distributions will have any notable overlap (e.g. for a Gaussian encoder, the means will most likely be very many standard deviations apart), presuming a sensible latent space is being learned. Consequently, even though this second term is unbiased and may have an expectation comparable or even larger than the first, it is heavily skewed—it is usually negligible, but occasionally large in the rare instances where there is substantial overlap between encodings.

Let the second term of (10b) be T_2 and the event that this is significant be E_S , such that $\mathbb{E}[T_2 \mid \neg E_S] \approx 0$. As explained above, $\mathbb{P}(E_S) \ll 1$ typically. We now have

$$\begin{aligned} \mathbb{E}[\hat{\mathbf{H}}] &= \mathbb{P}(E_S) \mathbb{E}[\hat{\mathbf{H}} \mid E_S] + (1 - \mathbb{P}(E_S)) \mathbb{E}[\hat{\mathbf{H}} \mid \neg E_S] \\ &= \mathbb{P}(E_S) \mathbb{E}[\hat{\mathbf{H}} \mid E_S] + (1 - \mathbb{P}(E_S)) \\ &\quad \cdot (\log n - \frac{1}{B} \sum_{b=1}^B \mathbb{E}[\log q_\phi(\mathbf{z}_b \mid \mathbf{x}_b) \mid \neg E_S] - \mathbb{E}[T_2 \mid \neg E_S]) \\ &= \mathbb{P}(E_S) \mathbb{E}[\hat{\mathbf{H}} \mid E_S] + (1 - \mathbb{P}(E_S)) \\ &\quad \cdot (\log n - \mathbb{E}[\log q_\phi(\mathbf{z}_1 \mid \mathbf{x}_1) \mid \neg E_S] - \mathbb{E}[T_2 \mid \neg E_S]) \\ &\approx \mathbb{P}(E_S) \mathbb{E}[\hat{\mathbf{H}} \mid E_S] \\ &\quad + (1 - \mathbb{P}(E_S)) (\log n - \mathbb{E}[\log q_\phi(\mathbf{z}_1 \mid \mathbf{x}_1)]) \end{aligned}$$

where the approximation relies firstly on our previous assumption that $\mathbb{E}[T_2 \mid \neg E_S] \approx 0$ and also that $\mathbb{E}[\log q_\phi(\mathbf{z}_1 \mid \mathbf{x}_1) \mid \neg E_S] \approx \mathbb{E}[\log q_\phi(\mathbf{z}_1 \mid \mathbf{x}_1)]$. This second assumption will also generally hold in practice, firstly because the occurrence of E_S is dominated by whether two similar datapoints are drawn (rather than by the value of \mathbf{x}_1) and secondly because $\mathbb{P}(E_S) \ll 1$ implies that

$$\begin{aligned} &\mathbb{E}[\log q_\phi(\mathbf{z}_1 \mid \mathbf{x}_1)] \\ &= (1 - \mathbb{P}(E_S)) \mathbb{E}[\log q_\phi(\mathbf{z}_1 \mid \mathbf{x}_1) \mid \neg E_S] \\ &\quad + \mathbb{P}(E_S) \mathbb{E}[\log q_\phi(\mathbf{z}_1 \mid \mathbf{x}_1) \mid E_S] \\ &\approx \mathbb{E}[\log q_\phi(\mathbf{z}_1 \mid \mathbf{x}_1) \mid \neg E_S]. \end{aligned}$$

Characterising $\mathbb{E}[\hat{\mathbf{H}} \mid E_S]$ precisely is a little more challenging, but it can safely be assumed to be smaller than $\mathbb{E}[\log q_\phi(\mathbf{z}_1 \mid \mathbf{x}_1)]$, which is approximately what would result from all the \mathbf{x}'_b being the same as \mathbf{x}_b . We thus see that even when the event E_S does occur, the resulting gradients will still, at most, be on a comparable scale to when it does not. Consequently, whenever E_S is rare, the $(1 - \mathbb{P}(E_S)) \mathbb{E}[\hat{\mathbf{H}} \mid \neg E_S]$ term will dominate and we thus have

$$\begin{aligned} \mathbb{E}[\hat{\mathbf{H}}] &\approx \log n - \mathbb{E}[\log q_\phi(\mathbf{z}_1 \mid \mathbf{x}_1)] \\ &= \log n + \mathbb{E}_{p(\mathbf{x})}[\mathbf{H}[q_\phi(\mathbf{z} \mid \mathbf{x})]]. \end{aligned}$$

More significantly, we see that the estimator mimics the β -VAE regularisation up to a constant factor $\log n$, as adding the $\mathbb{E}_{q(\mathbf{z})}[\log p(\mathbf{z})]$ back in gives

$$\begin{aligned} &-\mathbb{E}[\hat{\mathbf{H}}] - \mathbb{E}_{q(\mathbf{z})}[\log p(\mathbf{z})] \\ &\approx \mathbb{E}_{p(\mathbf{x})}[\text{KL}(q_\phi(\mathbf{z} \mid \mathbf{x}) \parallel p(\mathbf{z}))] - \log n. \end{aligned}$$

We should thus expect to empirically see training with this estimator as a regulariser to behave similarly to the β -VAE with the same regularisation term whenever $B \ll n$. Note that the $\log n$ constant factor will not impact the gradients, but does mean that it is possible, even likely, that negative estimates for $\hat{\mathbf{K}}\mathbf{L}$ will be generated, even though we know the true value is positive.

Overcoming the problem can, at least to a certain degree, be overcome by using very large batch sizes B , at an inevitable computational and memory cost. The problem is potentially exacerbated in higher dimensional latent spaces and larger datasets, for which one would typically expect the typical overlap of datapoints to decrease.